

Activated Hopping, Barrier Fluctuations, and Heterogeneity in Glassy Suspensions and Liquids[†]

Kenneth S. Schweizer* and Erica J. Saltzman

Departments of Materials Science and Chemistry and Frederick Seitz Materials Research Laboratory,
University of Illinois, 1304 West Green Street, Urbana, Illinois 61801

Received: May 24, 2004; In Final Form: August 12, 2004

Our entropic barrier hopping theory of glassy hard sphere colloidal suspensions is extended to include heterogeneity within a simple trap model framework. The origin of local domains, their size, and the corresponding static barrier fluctuations are attributed to mesoscopic density fluctuations of an amplitude controlled by the bulk compressibility. Based on typical values of the density fluctuation correlation length in dense liquids, the domain size on which correlated hopping occurs is estimated to be 3–4 particle or molecular diameters. Consequences of barrier fluctuations include an increased average relaxation time, faster diffusion, stretched exponential relaxation, diffusion-viscosity decoupling, and a fractional Stokes–Einstein relation. The common origin of the fluctuation effects is the heterogeneity-induced component of the barrier. For colloidal suspensions in the typically studied volume fraction regime the barrier fluctuations have modest consequences, but significantly larger effects are predicted in the putative glassy regime. A statistical dynamical analysis of domain lifetime suggests that for suspensions the relaxation time of mesoscopic collective density fluctuations is at least as long as the single particle hopping time. A general, model-independent analysis of the single molecule incoherent dynamic structure factor for suspensions and thermal liquids has also been performed in the long time and intermediate wavevector regime. The coupling of single particle density and longitudinal stress fluctuations results in a wavevector-dependent apparent diffusion constant and a dynamic correlation length scale which is strongly temperature dependent and directly related to the translation-rotation decoupling factor. This dynamic length is estimated to be 10 times larger than a molecular diameter for tris-naphthyl benzene near the glass transition temperature but shrinks to a molecular size above the crossover temperature that signals the emergence of collective barriers.

I. Introduction

Slow dynamics in glass-forming materials remains a poorly understood problem of major scientific interest.^{1,2} Many vastly different theoretical approaches are vigorously debated. The idealized mode-coupling theory (IMCT) is an ambitious kinetic microscopic approach formulated at the level of molecules and forces which assumes the key slow process is local (cage scale) dynamic collective density fluctuations.^{3,4} A self-consistent mean field description is developed based on factorization of multi-point correlation functions. An impressive number of results for transport coefficients and wavevector dependent time correlation functions have been obtained. The prediction of an “ideal” nonergodicity or glass transition plays a central role. The hard sphere colloidal suspension is the system for which MCT has been most microscopically and quantitatively applied with considerable success.^{3,5,6}

“Schematic” formulations of IMCT have been used to interpret experiments on many thermal glass forming liquids.³ A major problem is that the predicted critical power law divergence of the alpha relaxation time at a temperature T_c is not observed. This divergence is generally agreed to be an unphysical consequence of the approximations of IMCT which appear to limit the theory to a “precursor” regime in which relaxation times increase by roughly 3–4 orders of magnitude.^{1–7}

However, in the deeply supercooled regime there is ample experimental evidence for a smooth dynamical crossover where changes in the temperature dependence of the alpha relaxation time, stretched exponential relaxation, bifurcation of the alpha and beta processes, onset of translation-rotation decoupling, and other phenomena occur at nearly the same empirically deduced temperature.^{1–7} The crossover temperature is often referred to as T_c , and is typically a factor of 1.1–1.4 larger than the glass transition temperature T_g . A common interpretation of T_c is that it signals a crossover to strongly activated dynamics, the neglect of which is associated with the failure of IMCT in the deeply supercooled regime.^{3,8} At these low temperatures, particles reach local minima in an energy landscape in a finite time, and long time motion is controlled by activated dynamics.⁸ This idea has motivated the construction of phenomenological “trap models.”^{8–11}

Experimental study of the activated dynamics regime in colloidal suspensions is severely impeded by the large elementary Brownian time scale.¹² Typically a factor of only 10^4 increase in relaxation time is accessible between the freezing transition and the kinetic vitrification volume fraction ($\phi_g \approx 0.57–0.58$).^{5,6,13} Computer simulations are also generally limited to studying the initial 3–4 decades of glassy dynamics.^{1,2,14,15} The development of confocal microscopy partially surmounts this obstacle for micron sized particle suspensions.^{16,17} Recent studies on suspensions beyond ϕ_g do see evidence of significant mobility and diffusive transport.^{16,17}

* Corresponding author. E-mail: kschweiz@uiuc.edu.

[†] Part of the special issue “Frank H. Stillinger Festschrift”.

Very recently, we developed a microscopic theory for entropic barrier formation and activated transport in hard sphere colloidal suspensions which “goes beyond” the simplest version of MCT while retaining many of its predictive features.^{18,19} The concept of an ideal glass transition plays no role, and activated hopping processes restore ergodicity at long times. Dynamical slowing down is a continuous, albeit precipitous, process with increasing fluid volume fraction. No adjustable parameter comparisons of the theory with experimental measurements of single particle dynamics and transport coefficients reveal good agreement.^{18,19} A new physical picture is suggested in which hopping over entropic barriers of size $\sim 7-8 k_B T$ at the kinetic glass transition volume fraction is responsible for the slow dynamics.

Interestingly, recent computer simulation studies^{20,21} of thermal and hard sphere like fluids find activated barrier hopping between “metabasins” commences close to the *theoretically predicted* MCT dynamic critical point (temperature or volume fraction) and is dominant in the system parameter range associated with the early stages of glassy dynamics. This has led to the suggestion the IMCT nonergodicity transition represents an “onset” temperature (volume fraction) T_A or T_0 for activated dynamics, which is higher (lower) than the critical temperature $T_c(\phi_c)$ deduced from empirical fitting and extrapolation of MCT formulas to experimental or simulation data.^{20,21} These simulation findings are in qualitative accord with our theoretical results and approach.

An obvious limitation of our prior theory^{18,19} is that “heterogeneity”^{1,22–24} effects are not explicitly taken into account. Very small deviations (“decoupling”) of the product of the self-diffusion constant and shear viscosity from its Stokes–Einstein value are predicted.¹⁹ Stretched exponential relaxation of dynamic correlators is not captured since the theory focuses on the mean barrier and hopping time.

The first goal of this paper is to generalize our approach to address heterogeneity issues within the simplest activated hopping/static disorder framework. The consequences for hard sphere suspensions are compared with the analogous behavior in thermal liquids. The second goal is to investigate the validity of the static disorder model and corresponding collective relaxation. Specifically, the spatial nature and temporal stability of mesoscopic scale density fluctuations, which define domains and induce a distribution of barriers and hopping times, are generically investigated using well-known time-dependent statistical dynamical methods. Finally, an analysis relevant to *both* overdamped colloidal suspensions and thermal glass forming liquids is carried out for the influence of heterogeneity and translation-rotation decoupling on the incoherent dynamic structure factor and an apparent growing *dynamic* length scale.

The paper is structured as follows. In section II, our theory of entropic barrier hopping in hard sphere suspensions is briefly reviewed. New calculations and analysis of the glassy shear modulus are also presented. A simple static disorder model based on mesoscopic domains is discussed in section III and applied to compute various dynamical properties. A generic analysis of collective and single particle dynamic structure factors at long times and on mesoscopic length scales is presented in section IV and V, respectively. Applications to heterogeneity issues for both glassy suspensions and thermal liquids are given. The paper concludes in section VI with a brief summary and discussion.

II. Entropic Barriers and Activated Hopping in Colloidal Suspensions

A. Microscopic Theory. Our theory for the slow dynamics of hard sphere suspensions has been described in detail

elsewhere.^{18,19} The starting point is the “naïve” version of IMCT²⁵ which focuses on tagged particle motion. The central object is the force-force time correlation function, or dynamic friction, exerted on a particle by its surroundings:^{18,25}

$$K(t) = \langle \vec{F}(0) \cdot \vec{F}(t) \rangle = \frac{1}{3} \beta^{-2} \int \frac{d\vec{q}}{(2\pi)^3} q^2 C^2(q) \rho S(q) \Gamma_s(q, t) \Gamma_c(q, t) \quad (1)$$

Here ρ is the fluid number density, $\vec{F}(t)$ is the total force exerted on a tagged particle by the surrounding fluid at time t , and β is the inverse thermal energy. $C(q)$ is the Fourier transform of the direct correlation function and $S(q)$ the dimensionless collective structure factor.²⁶ Percus–Yevick (PY) theory is employed to compute the required equilibrium correlation functions. The “propagator” $\Gamma_s(q, t)$ ($\Gamma_c(q, t)$) is the $t = 0$ normalized single particle (collective) dynamic structure factor which in fluids decays to zero at long times, but is nonzero in a glass. The long time nonzero values of the propagators, or Debye–Waller factors, describe localized single particle and collective density fluctuations in a harmonic or Einstein model of the amorphous solid state:^{18,25}

$$\Gamma_s(q, t \rightarrow \infty) = \exp(-q^2/4\alpha)$$

$$\Gamma_c(q, t \rightarrow \infty) = \exp(-q^2/4\alpha S(q)) \quad (2)$$

An ensemble-averaged “localization length” is defined as

$$r_L^2 \equiv 3/2\alpha \quad (3)$$

A self-consistent equation for this dynamic order parameter can be straightforwardly derived:^{18,25}

$$\alpha = \frac{1}{2} \beta^2 K(t \rightarrow \infty) = \frac{1}{6} \int \frac{d\vec{q}}{(2\pi)^3} \rho q^2 C^2(q) S(q) \exp(-(q^2/4\alpha)(1 + S^{-1}(q))) \quad (4)$$

Based on PY theory²⁶ input, a localization transition occurs¹⁸ at $\phi_{\text{MCT}} \equiv \phi_c = 0.432$ corresponding to the naïve IMCT glass transition which lies below the full IMCT-PY value of 0.515.^{3,4}

To treat activated processes, the IMCT nonergodicity transition is interpreted as signaling the emergence of finite barriers in a *dynamically defined* landscape and strong *transient* localization. MCT is a theory for ensemble-averaged time correlation functions, and to go beyond it a stochastic equation of motion (EOM) is constructed for the *non-ensemble* averaged single particle *dynamical variable*, $r(t)$, which represents the displacement of a particle from a random initial location. Three aspects enter.¹⁸ (1) The short time motion is Fickian diffusion.¹² (2) In the absence of thermal fluctuations, IMCT is assumed to correctly predict the tendency to localize in a cage. Hence, in the deterministic limit the naïve IMCT localization condition should be recovered. This idea guides the construction of a *displacement-dependent* effective caging force, $-\partial F/\partial r$, which at high volume fraction favors localization. F is called a nonequilibrium “effective free energy” but does *not* have any rigorous equilibrium meaning. (3) Ergodicity restoring fluctuations destroy the naïve IMCT glass transition via activated hopping.

The resulting nonlinear Langevin equation in the overdamped limit corresponds to a force balance¹⁸

$$-\zeta_s \frac{d}{dt} r - \frac{\partial}{\partial r} F + \delta f = M \frac{d^2}{dt^2} r = 0 \quad (5)$$

where ζ_s is the short time friction constant due to hydrodynamic pair interactions or binary collisions. Based on the latter, $\zeta_s = \zeta_0 g(\sigma)$, where $\zeta_0 = k_B T / D_0 = 3\pi\sigma\eta_0$ is the Stokes–Einstein friction constant,²⁷ η_0 is the solvent viscosity, and $g(\sigma)$ is the contact value of the radial distribution function.^{26,28} The use of two particle hydrodynamics to quantify the short time friction constant yields nearly identical results.^{18,19} The white noise fluctuating force is statistically uncorrelated with the tagged particle position and velocity and satisfies $\langle \delta f(0) \delta f(t) \rangle = 6\beta^{-1} \zeta_s \delta(t)$.

The effective “free energy” function (in units of $k_B T$ on a per particle basis) quantifies the difference between localized (nonzero α) and delocalized ($\alpha = 0$) states. It is constructed in the spirit of density functional theory²⁹ (DFT)

$$F(\alpha) = \frac{3}{2} \ln(\alpha) - \int \frac{d\vec{q}}{(2\pi)^3} \rho C^2(q) S(q) [1 + S^{-1}(q)]^{-1} \exp\left(-\frac{q^2}{4\alpha} (1 + S^{-1}(q))\right) \equiv F_0 + F_I \quad (6)$$

The leading “ideal” term favors the fluid state and is of a harmonic solid form.²⁵ The second “interaction” contribution corresponds to an entropic trapping potential favoring localization. The order parameter $\alpha(t)$, or its analogue $r(t) = (3/2\alpha(t))^{1/2}$, is now a *nonaveraged* dynamical variable. Minimization of eq 6 with respect to α , or solution of eq 5 in the absence of noise, by construction yields the naïve IMCT localization condition of eq 4. For $\phi > \phi_c$, an intensive entropic barrier, F_B , and local minimum appear in $F(r)$ as shown in Figure 1. Characteristic lengths include the location of the minimum (“localization length”, r_L , from eqs 3 and 4), local maximum (barrier location), r_B , and a “diffusion length” defined as the displacement, $L_D \sim \sigma$, beyond which the interaction part of the caging force is negligible.¹⁸ As previously discussed,¹⁸ we make no claim to a “rigorous” derivation of our approach.

Equations 1, 2, 5, and 6 imply the caging force evolves in time via single particle and collective motions. However, collective motion is treated within a Vineyard type approximation for the collective propagator which neglects explicit many particle dynamics, a simplification which is quite accurate on local scales.^{25,26} In this sense, our approach is a dynamical mean field theory. The caging force is self-consistently and nonlinearly coupled with single particle motion and hence contains elements of the “dynamic facilitation” idea³⁰ since evolution of the dynamic order parameter is state (displacement)-dependent.

It should be emphasized that our theory is built on a nonequilibrium “free energy” or dynamical caging force from which an entropic barrier to transport emerges. It is distinct from, and vastly simpler than, simulation based energy landscape approaches.

The entropic barrier as a function of the inverse dimensionless compressibility,²⁶ $S(q=0) \equiv S_0 = (1 - \phi)^4 / (1 + 2\phi)^2$, is shown in the inset of Figure 1. Except very near the crossover volume fraction, the barrier is a remarkably linear function given by

$$F_B \cong \frac{0.077}{S_0} - 3.51 \quad (7)$$

which applies up to high ϕ . This result implies a surprisingly strong connection between the long wavelength thermodynamic measure of density fluctuations, and the entropic barrier

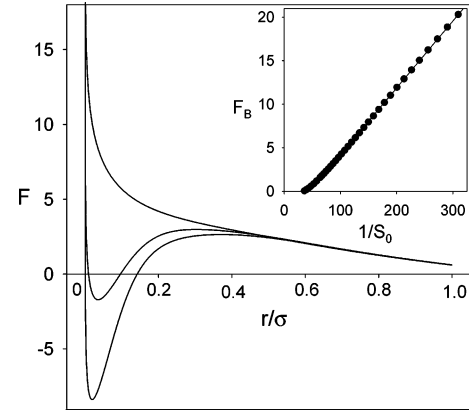


Figure 1. “Effective nonequilibrium free energy” (in units of $k_B T$) as a function of reduced hard sphere displacement for volume fractions (from top): $\phi = 0.3, 0.55$, and 0.6 . The inset shows the entropic barrier (points) as a function of the inverse dimensionless compressibility. The linear fit given in eq 7 is also shown.

computed using the fully microscopic cage correlations. Whether such a connection persists all the way up to random close packing (RCP) at $\phi_{RCP} \cong 0.64$ (or the “maximally random jammed” state at $\phi_{MRJ} \cong 0.6331$) where $1/S_0$ diverges is not known since the PY structural input does not properly describe the jamming.

The mean barrier hopping time, $\bar{\tau}$, is closely correlated with the alpha or structural relaxation time. In the overdamped limit, where barrier crossing is a diffusive process, Kramers theory³² yields¹⁸

$$\frac{\bar{\tau}}{\tau_0} = \frac{2\pi g(\sigma)}{(K_0 K_B)^{1/2}} e^{F_B} \quad (8)$$

where $\tau_0 = \sigma^2 \zeta_0 / k_B T$ is an elementary Brownian diffusion time, and K_0 and K_B are the absolute magnitudes (in units of $1/\beta\sigma^2$) of the harmonic curvatures of the minimum and barrier of $F(r)$, respectively. Transport coefficients are computed using Green-Kubo formulas and the MCT factorization approximation.^{3,26} The shear viscosity is given by¹⁹

$$\eta = \eta_\infty + \frac{k_B T}{120\pi^2} \int_0^\infty dq q^2 \left(\frac{\partial}{\partial q} \ln S(q) \right)^2 \frac{1}{D_s^c(q)} \quad (9)$$

where $\eta_\infty = \eta_0 g(\sigma)$ is the high-frequency viscosity, the cage diffusion constant³³ is

$$D_s^c(q) = \frac{D_0}{S(q)[g(\sigma)d(q)^{-1} + (\zeta_{HOP}/\zeta_0)]} \quad (10)$$

with $d(q) = [1 - j_0(k\sigma) + 2j_2(k\sigma)]^{-1}$ where $j_k(x)$ is the spherical Bessel function of order k , and the friction constant is a sum of the short time and a hopping contribution

$$\zeta_{HOP} = k_B T / D_{HOP} = 6k_B T \bar{\tau} / L_D^2 \quad (11)$$

No adjustable parameter calculations of the single particle relaxation time, shear viscosity, self-diffusion constant, and other quantities have been shown^{18,19} to be in very good agreement with experiments up to $\phi \sim 0.57$ – 0.58 . For several reasons, including the quantitative limitations of the PY input, the essentially quantitative agreement between our theory and experiment is rather surprising.

B. Glassy Elastic Modulus. The elastic shear modulus follows from the Green-Kubo formula^{3,33}

$$G' = \beta \rho \sum_{ij} \langle x_i(0) f_i^z(0) x_j(t \rightarrow \infty) f_j^z(t \rightarrow \infty) \rangle \cong \frac{k_B T}{60\pi^2} \int_0^\infty dq \left(q^2 \frac{\partial}{\partial q} \ln S(q) \right)^2 \exp(-q^2/2S(q)\alpha) \quad (12)$$

where $x_j f_j^z$ is a microscopic shear stress variable given by the product of the x component of the position of particle j and the total force acting on it. The second line employs the standard MCT factorization and projection approximations,^{3,26} and the localization parameter α is computed from eq 4. Equation 12 is the standard IMCT result.³ Results for the nondimensionalized G' (units of $k_B T \sigma^{-3}$) are shown in Figure 2 and are well described by several relations

$$G' \cong 0.00164 e^{25.9\phi} \cong 0.573 \phi \left(\frac{\sigma}{r_L} \right)^2 \cong 0.00412 S_0^{-2.35} \quad (13)$$

As previously discussed in the context of depletion gels,³⁴ the modulus is inversely related to the square of the localization length which is given accurately by $r_L \cong 29.9\sigma \exp(-12.2\phi)$.¹⁸ This result has been rationalized based on qualitative mechanics arguments.³⁵ The final equality in eq 13 demonstrates the modulus depends on the dimensionless compressibility in an interesting power law fashion. This is again surprising since it is the high wavevector, microscopic cage scale fluctuations in eq 12 that dominate the modulus calculation. As discussed elsewhere,³⁶ the magnitude and volume fraction dependence of G' is in quite good accord with experiments on hard sphere suspensions.^{37–39}

The glassy longitudinal modulus, M' , is given by⁴⁰

$$M' = \beta \rho \sum_{ij} \langle z_i(0) f_i^z(0) z_j(t \rightarrow \infty) f_j^z(t \rightarrow \infty) \rangle \cong 3G' \quad (14)$$

The approximate equality follows from the MCT factorization and projection onto bilinear products of density fluctuations approximations.^{3,4} The inset of Figure 2 shows the ratio of the longitudinal and bulk ($K_B = \rho k_B T / S_0$) moduli

$$\Gamma \equiv \frac{M'}{K_B} = \frac{\pi}{2\phi} S_0 \tilde{G}' \quad (15)$$

This ratio is a monotonically, but relatively weakly, increasing function of volume fraction. Near the kinetic glass transition, it is ~ 10 , which has consequences for the question of heterogeneous domain lifetime addressed in section IV.

III. Spatial Heterogeneity and Static Barrier Fluctuations

Our approach to including “heterogeneity” within the context of an activated barrier hopping theory builds on the enormous amount of prior work based on (effectively) static domain disorder or trap models.^{8–11} These models have been fruitfully applied to slow dynamics problems in structural glasses, spin glasses, protein folding, and exciton or charge transport. Such trap models generally invoke a static distribution (often Gaussian) of barriers which yield a distribution of relaxation times. Most prior implementations have been phenomenological in three respects: (a) fundamental justification of the effectively “static” aspect of disorder is lacking; (b) the physical origin of domains, their size, and the underlying crucial variable(s) that determine barrier fluctuations, are not specified; and (c) the key Gaussian barrier fluctuation parameter (variance) is treated as empirical input. Although the theory proposed in this section is in the spirit of prior trap-like models, we have striven to relax

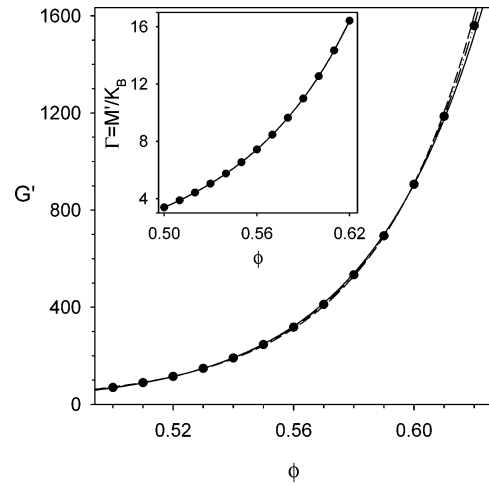


Figure 2. Dimensionless elastic shear modulus (in units of $k_B T \sigma^{-3}$) as a function of volume fraction (points). Curves are various fits: $G' = 0.00164 e^{25.9\phi}$ (solid); $G' = 0.573\phi/r_L\sigma^2$ (dash-dot); $G' = 0.00412 S_0^{-2.347}$ (dashed). All fits are nearly perfect and identical to each other up to $\phi \sim 0.61$. The inset shows the ratio of the longitudinal and bulk moduli as a function of volume fraction. The curve through the data points is a guide to the eye.

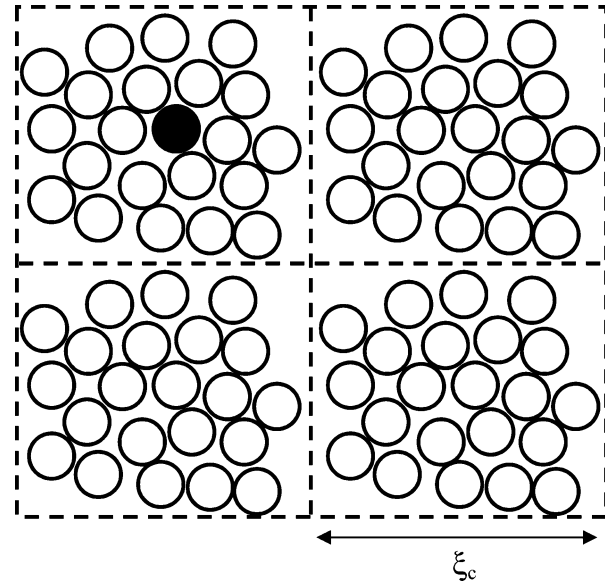


Figure 3. Schematic of mesoscopic domains of diameter ξ_c .

limitations (b) and (c), and no (or minimal) adjustable parameter quantitative applications are pursued. Point (a) is studied in section IV.

A. Model Formulation and Heterogeneity Length Scale.

Three related issues are relevant to going beyond our dynamical mean field theory description. We address them in a manner applicable to both colloidal suspensions and thermal liquids.

First, in a dense and deeply supercooled fluid ($\phi > \phi_c, T < T_c$), the discrete elementary activated hopping event on the particle radius length scale is possible only via cooperative many particle motions. A characteristic “cooperativity” length scale, ξ_c , for correlated hopping dynamics is commonly envisioned¹ (see Figure 3). As a *consequence*, so-called “dynamic heterogeneities” are expected to emerge which we define in this section as simply local domains with different relaxation times. We do not explicitly address many particle dynamic cooperativity in this paper, and in contrast to Adams-Gibbs and some other models,¹ we do *not* associate glassy slowing down with growth of ξ_c . Moreover, the effective glassy barrier for such an intradomain

cooperative hopping process is assumed to be well approximated by our prior mean field approach.^{18,19} However, recognition of the existence of a dynamical domain structure when $\phi > \phi_c$ or $T < T_c$ implies a distribution of (hopping) relaxation times due to the (finite size) fluctuations of structural and/or thermodynamic properties which determine the barrier in our theory.

The second issue is the size, and physical origin, of the mesoscopic domains. Since our approach is based on density fluctuations (as is MCT), the natural key fluctuating variable is the density in a volume $V_c \equiv (\pi/6)\xi_c^3$. In the spirit of strong coupling of structure and dynamics, the domain diameter is related to twice the density fluctuation-density fluctuation correlation length, ξ_ρ , as

$$\xi_c \cong 2(\sigma + \xi_\rho) \quad (16)$$

where σ enters due to hard core impenetrability. This is the appropriate length scale to render domains statistically independent in equilibrium. In dense fluids, ξ_ρ is defined from the accurate Yukawa form for the oscillatory density fluctuation correlation function^{26,41}

$$S(r) \propto \frac{\sigma}{r} \exp(-r/\xi_\rho) \sin(2\pi r/\sigma + \theta), \quad r > \sigma \quad (17)$$

For dense atomic and flexible polymer liquids interacting via repulsive forces, both integral equation theory and molecular dynamics simulations⁴¹ find $\xi_\rho/\sigma \approx 0.5-1$. Equation 16 thereby yields a domain diameter of $\xi_c/\sigma \approx 3-4$. Although this estimate is neither rigorous nor without modest ambiguity, it seems physically reasonable and our subsequent model calculations will employ it.

For thermal liquids, the length ξ_c is estimated in an identical manner. A molecular diameter is computed from the molar volume or liquid density under the assumption of spherical geometry (as done in the analysis of 4-d nuclear magnetic resonance (NMR) measurements^{22-24,42,43}). For *o*-terphenyl (OTP) $\sigma \approx 0.75$ nm, implying a cooperativity length or domain diameter of $\sim 2.3-3$ nm, consistent with NMR measurements near T_g .²² However, whether the NMR “dynamic heterogeneity length” is equivalent to our “cooperativity” length or domain diameter is not clear²² so the apparent good numerical agreement may be accidental. Thus, it is instructive to estimate ξ_c for other molecular liquids. The calculation is elementary since an effective diameter scales as the cube root of molecular mass and most organic liquids have nearly the same mass density. This implies diameters of $\sigma \sim 1, 0.5, 0.64$ and 1 nm for tri-naphthyl-benzene (TNB), glycerol (G), sorbitol (S), and poly-vinyl acetate (PVAC). For the polymer, the appropriate unit is identified with the Kuhn length,⁴⁴ which for PVAC corresponds to ~ 10 backbone bonds or 5 monomers. These numbers imply: $\xi_c \sim 3-4$ (TNB), $1.5-2$ (G), $2-2.6$ (S), and $3-4$ (PVAC) nanometers. NMR measurements near T_g find 1.2 ± 0.5 (G), 2.5 ± 1 (S), and 3.5 ± 1 (PVAC) nm, which are all in agreement with the theoretical estimates to within the significant experimental error bars.

The above discussion assumes the domain diameter or cooperativity length relevant to the hopping process is, to a first approximation, volume fraction and temperature independent. This speculative but simplifying idea has been successfully applied in polymer melts and blends^{44,45} where the relevant length scale is identified with an equilibrium measure of chain stiffness, the Kuhn length. It is demonstrated in section V that this simplification does *not* imply that *dynamical* correlation

lengths extracted from ensemble-averaged time correlation functions are temperature independent.

On the mesoscopic $3-4 \sigma$ length scale, the static structure factor of high volume fraction suspensions or dense thermal liquids is essentially featureless and wavevector independent.²⁶ Hence, the density fluctuations within domains can be estimated from knowledge of the bulk compressibility²⁶

$$\langle (\delta\rho)^2 \rangle = \frac{\rho S_0}{V_c} \quad (18)$$

Our prior theory^{18,19} is recovered in the $V_c, \xi_c \rightarrow \infty$ limit. The use of bulklike density fluctuations (or a different local thermodynamic variable such as entropy) to distinguish dynamically distinct domains has been employed by many different workers.^{1,22,23,46-48} Volume fraction fluctuations are Gaussian

$$P(\phi) \propto \exp(-(\phi - \bar{\phi})^2/2\langle (\delta\phi)^2 \rangle) \quad (19)$$

$$\langle (\delta\phi)^2 \rangle = \phi S_0 \frac{V_m}{V_c} \equiv \phi S_0 \left(\frac{\sigma}{\xi_c} \right)^3 \quad (20)$$

where V_m is the molecular volume. This does not rigorously imply Gaussian distributions of the hopping time or entropic barrier. However, motivated by the simple trap and random energy models,⁸⁻¹⁰ we also consider a second approach corresponding to a Gaussian distribution of barriers, i.e., $F_B(\phi) \cong \bar{F}_B + (\partial F_B/\partial \phi)\phi(\phi - \bar{\phi})$ where $\bar{\phi}$ is the bulk volume fraction and \bar{F}_B is the corresponding mean barrier. One could view this as a simplifying mathematical approximation. Alternatively, a Gaussian barrier distribution could be more physically appropriate than eq 19. The only required information is the second moment or barrier variance

$$P(F_B) \propto \exp(-(F_B - \bar{F}_B)^2/2\sigma_E^2) \quad (21)$$

$$\sigma_E^2 = \frac{V_m \phi S_0}{V_c} \left(\frac{\partial F_B}{\partial \phi} \right)^2$$

Equation 21 may be valid for at least two reasons: (i) density fluctuations are small at high density or low temperatures, and (ii) barriers may be determined by a sufficient number of interparticle interactions that a central limit theorem argument applies. Recent computer simulation landscape analyses suggest the height of barriers separating megabasins are statistically well described by a Gaussian distribution.²¹ Hence, eq 21 may be more accurate than its naïve motivation. Also, recent experiments⁴⁹ claim strong support for the existence of *correlated nanoscale thermodynamic and relaxation time fluctuations* which also suggests the potential usefulness of the above approach.

The third issue is the domain lifetime. We adopt the simplifying assumption that on the time scales of interest the domain pattern is static.⁴⁶⁻⁴⁸ This requires that collective dynamic density fluctuations on the ξ_c scale relax more slowly than the process of interest. Near the glass transition in thermal liquids, single molecule rotational diffusion,⁵⁰ photochemical deep bleach,⁵¹ and solvation dynamics⁵² experiments all find a “heterogeneity lifetime” or “environmental exchange time” one or more orders of magnitude longer than the ensemble-averaged alpha relaxation time. NMR^{22,42} and some dielectric relaxation⁵³ experiments find the exchange time is comparable to the average alpha relaxation time.

B. Modulus, Relaxation Times, and Diffusion-Viscosity Decoupling. Within the static disorder model the ensemble

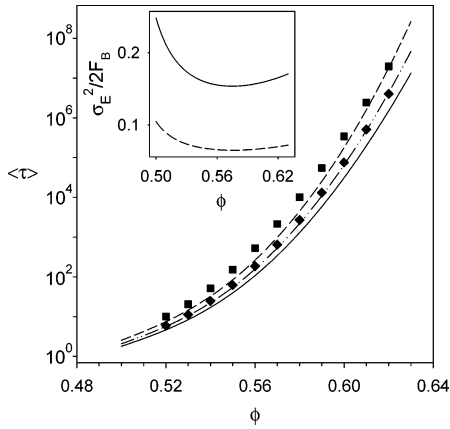


Figure 4. Ensemble-averaged hopping time (in units of $\tau_0 \equiv \beta\sigma^3\xi_0$) as a function of volume fraction. The main frame shows the mean relaxation time $\bar{\tau}$ (solid curve), Gaussian barrier fluctuation model time with $\xi_c/\sigma = 4$ (dash-dot) and $\xi_c/\sigma = 3$ (dashed), and the full volume fraction fluctuation averaged time, $\langle \tau \rangle$, with $\xi_c/\sigma = 4$ (diamonds) and $\xi_c/\sigma = 3$ (squares). Inset shows the ratio of the fluctuation-induced barrier to the mean barrier as a function of volume fraction for $\xi_c/\sigma = 4$ (dashed curve) and $\xi_c/\sigma = 3$ (solid curve).

average of any observable W is given by

$$\langle W \rangle \cong \int_{\phi_{\min}}^{\phi_{\max}} d\phi' P(\bar{\phi} - \phi') W(\phi') \quad (22)$$

The lower limit is chosen to be 0.5 since below this volume fraction entropic barriers are less than $k_B T$ and a hopping picture is not valid.¹⁸ Our results are not sensitive to modest adjustments of this lower limit. The upper limit is chosen to be the maximum volume fraction (incompressible state) which in PY theory corresponds to $\phi_{\max} = 1$. Of course, PY theory is not accurate as the true (RCP-like) incompressible state is approached. Hence, in subsequent figures, we present calculations only up to volume fractions for which we have explicitly verified relative insensitivity to the upper limit in eq 22. For example, for $\phi = 0.6$ and $\xi_c/\sigma = 3$, varying ϕ_{\max} from 0.64 to 1 results in a $\sim 13\%$ change in $\langle \tau \rangle$.

The influence of local volume fraction fluctuations on the elastic shear modulus is found to be remarkably small (not shown). Changes relative to the mean field G' results in Figure 2 correspond to a 15% (4%) or less increase for $\xi_c = 3$ (4) σ over the range $\phi = 0.52$ –0.62.

Calculations of the average hopping time, $\langle \tau \rangle$, using eqs 19, 20, and 22 are given in Figure 4. Their analogue based on a Gaussian barrier distribution, in combination with ignoring the small effect of fluctuations on the prefactor in eq 8 (less than a factor of 2 over the range $\phi = 0.5$ –0.62), is also shown. This corresponds to the analytic Gaussian trap model formula^{8,48}

$$\langle \tau \rangle \cong \bar{\tau} \exp(\sigma_E^2/2) \quad (23)$$

where $\bar{\tau}$ is given by eq 8 and the variance by eq 21. Relaxation times are increased by domain density fluctuations and increasingly so as volume fraction increases. However, this is not a dramatic effect, with increases of the average hopping time being roughly an order of magnitude or less. Thus, prior comparisons^{18,19} of our dynamic mean field theory and experiment for the location of the kinetic glass transition, incoherent structure factor relaxation time, diffusion constant, and viscosity of hard sphere suspensions remain nearly unchanged to within the considerable experimental uncertainties. For example, for the experimental system of ref 6 we previously found¹⁸ $\phi_g = 0.578$ based on the kinetic definition of a glass as $\bar{\tau} = 10\,000$ seconds.

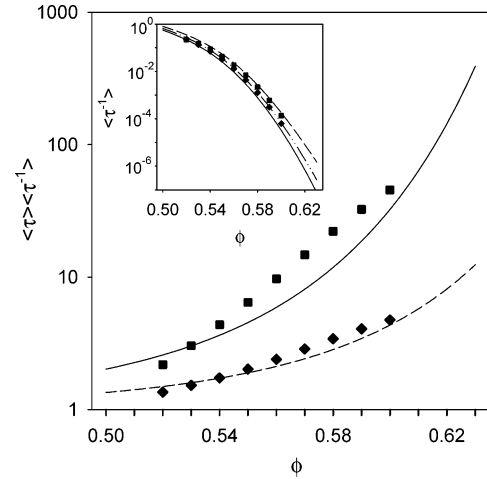


Figure 5. Decoupling parameter $\langle \tau \rangle \langle \tau^{-1} \rangle$ as a function of volume fraction for the Gaussian barrier fluctuation model with $\xi_c/\sigma = 4$ (dashed curve) and $\xi_c/\sigma = 3$ (solid curve), and based on the full volume fraction fluctuation averaged $\langle \tau \rangle$ and $\langle \tau^{-1} \rangle$ with $\xi_c/\sigma = 4$ (diamonds) and $\xi_c/\sigma = 3$ (squares). The inset shows the inverse relaxation time corresponding to the mean field result $\bar{\tau}^{-1}$ (solid curve), Gaussian barrier fluctuation model with $\xi_c/\sigma = 4$ (dash-dot curve) and $\xi_c/\sigma = 3$ (dashed curve), and the full averaged result for $\xi_c/\sigma = 4$ (diamonds) and $\xi_c/\sigma = 3$ (squares).

Including barrier fluctuations yields $\phi_g = 0.570$ (Gaussian barrier distribution) or $\phi_g = 0.565$ (full volume fraction fluctuations) for $\xi_c = 3\sigma$. The Gaussian barrier fluctuation based calculations yield somewhat smaller enhancements of $\langle \tau \rangle$ for most volume fractions but overall are in rather good agreement with calculations based on eqs 19 and 20. The inset in Figure 4 shows the ratio of the variance to the mean barrier. For the $\phi > 0.5$ regime of interest, this ratio is not highly variable, a result that will be important in the subsequent analysis.

The influence of mesoscopic density fluctuations on the self-diffusion constant can be estimated using a Fickian relation relevant to hopping transport

$$D_{\text{HOP}} \approx \sigma^2 \langle \tau^{-1} \rangle / 6 \quad (24)$$

Within the Gaussian trap model,⁸ $\langle \tau^{-1} \rangle \cong \bar{\tau}^{-1} \exp(\sigma_E^2/2)$. As discussed by many others,^{1,22,23,48} fluctuations increase the average relaxation *rate* relative to the most probable value thereby “speeding up” self-diffusion. Results are shown in the inset of Figure 5, and the effect of barrier fluctuations is comparable to that shown in Figure 4. The main frame of Figure 5 shows a “decoupling factor” defined as the product of the average relaxation time and its inverse

$$R \equiv \langle \tau \rangle \langle \tau^{-1} \rangle \cong \exp(\sigma_E^2) \quad (25)$$

The final expression in eq 25 is the analytic Gaussian trap model result. Experimentally, “translation-rotation (viscosity) decoupling” is quantified via the ratio^{22,23}

$$R_D \equiv \frac{D\eta}{(D\eta)_{\infty}} \quad (26a)$$

$$(D\eta)_{\infty} \cong (D\eta)_{\text{SE}} = (3\pi\sigma\beta)^{-1} \quad (26b)$$

where eq 26b refers to the high temperature “normal” liquid regime which is well described by the Stokes–Einstein result.²⁷ Physically, we expect $R \approx R_D$.

Figure 5 shows reasonably good agreement between the full volume fraction fluctuation calculation of R and its Gaussian

barrier analogue. The full calculations are rather well described by an exponential dependence on volume fraction which extrapolates to the mean field value of unity at $\phi \cong 0.50$ where the entropic barrier is $\sim k_B T$; the Gaussian trap model analogue is more strongly varying. Near the kinetic glass transition volume fraction, the decoupling factor is small, $R \sim 3-10$. Perhaps this rationalizes why the wavevector dependence of the incoherent dynamic structure factor,⁶ $F(q, t)$, is well described by a Fickian form, $\ln F(q, t) \propto -q^2$, for $q\sigma \cong 2.6-10$ up to $\phi \cong 0.58$. It also is consistent with the idea that such experiments are probing only the early stages, or precursor regime, of the slow alpha relaxation process. However, deeper in the “glass” much larger decoupling factors are calculated, e.g., $R \sim 420$ for $\phi \cong 0.63$ and $\xi_c = 3\sigma$ based on the Gaussian barrier fluctuation model. The nonGaussian calculation of R (which is more sensitive to the quantitative limitations of the PY input at very high ϕ) becomes smaller than its Gaussian analogue and more slowly increasing with volume fraction, as the ultrahigh ϕ regime is entered.

To compare the above results to experiments on thermal glass forming liquids, we first note that at T_g (defined as $\tau(T_g) = 100$ seconds) the alpha relaxation time is typically^{1,54} a factor of 10^8-10^{10} times the relaxation time at the empirically extracted “crossover temperature” T_c , $\tau(T_c) \sim 10^{-7 \pm 1}$ seconds.⁵⁴ In strong contrast, the dynamics has slowed much less at the kinetic glass transition of colloidal suspensions which is operationally defined⁵ as when the relaxation time exceeds $\sim 10\,000$ seconds. Based on both our prior theoretical work¹⁹ and experiments,^{13,17} the shear viscosity (diffusion constant) is only a factor of ~ 1000 (10^{-3}) larger (smaller) than its value at the crossover volume fraction of $\phi_c \cong 0.43$. Thus, the computed low values of R are consistent with thermal liquid behavior. Prior work¹⁹ shows an enhancement (suppression) of the viscosity or hopping time (diffusion constant) by a factor of $\sim 10^9$ (10^{-9}) occurs at $\phi \cong 0.63$, which is the relevant volume fraction regime for comparison with thermal liquids at T_g . For TNB, $R_D \sim 400$ at T_g .⁵⁵ The calculated value of $R \sim 420$ at $\phi \cong 0.63$ discussed above seems pleasingly consistent with, and no doubt fortuitously close to, the experimental result.

C. Fractional Stokes–Einstein Relations. An issue related to decoupling is the functional relationship between the viscosity and self-diffusion constant in the deeply supercooled, barrier-dominated regime. A variety of experiments report a “fractional Stokes–Einstein” relation

$$D \propto \eta^{-\nu} \quad (27)$$

where typically $\nu \approx 0.7 \pm 0.1$.^{1,22,23} This relation is well obeyed for TNB with $\nu \approx 0.77$ over roughly 8 orders of magnitude in variation of the diffusion constant.⁵⁵ Figure 6 presents relevant calculations for colloidal suspensions. Over at least 6 orders of magnitude, an excellent fractional power law behavior emerges based on the full calculation and its Gaussian barrier fluctuation analog

$$\langle \tau^{-1} \rangle \propto \langle \tau \rangle^{-\nu} \quad (28)$$

The exponents are $\nu \cong 0.77(0.73)$ and $\nu \cong 0.90(0.88)$ for the full (Gaussian model) calculations and $\xi_c/\sigma = 3$ and 4, respectively. Intriguingly, the former values agree very well with the TNB experiment.⁵⁵

Within the context of our approach, the origin of the fractional Stokes–Einstein behavior can be *qualitatively* understood from the Gaussian barrier fluctuation version of our theory. We first define a reduced “viscosity” as the ratio of $\langle \tau \rangle$ to its

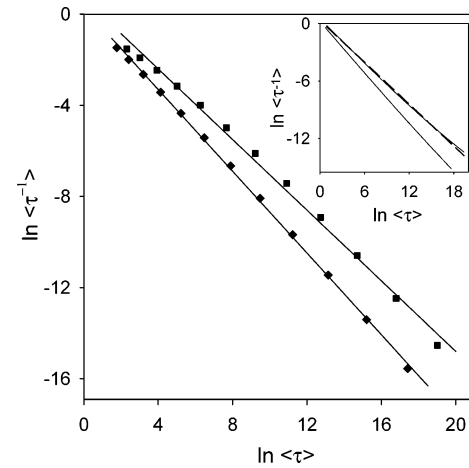


Figure 6. Demonstration of the power-law relation between $\langle \tau^{-1} \rangle$ and $\langle \tau \rangle$. The main frame shows the full volume fraction fluctuation results for $0.52 \leq \phi \leq 0.63$ ($\xi_c/\sigma = 3$ (squares) and 4 (diamonds)) with power-law fits (lines) characterized by exponents $\nu = 0.77$ and 0.90 for $\xi_c/\sigma = 3$ and 4, respectively. The inset shows the analogous Gaussian barrier fluctuation model results (solid curves). The dashed lines are power law fits with best fit exponents $\nu = 0.73$ and 0.88 for $\xi_c/\sigma = 3$ and 4, respectively.

“normal” fluid analogue (no barriers), τ_0 ⁵⁶

$$\tilde{\eta} \equiv \frac{\langle \tau \rangle}{\tau_0} \cong \exp(\bar{F}_B + \sigma_E^2/2) \quad (29)$$

where eq 23 has been used. Using eq 24, the corresponding reduced diffusion constant is

$$\tilde{D} \equiv \frac{\langle \tau^{-1} \rangle}{\tau_0^{-1}} \cong \exp(-\bar{F}_B + \sigma_E^2/2) \quad (30)$$

Equations 29 and 30 neglect “prefactors” involving the well and barrier curvatures in eq 8, the elastic modulus, and the hopping distance L_D . However, as discussed further below, all of these prefactors are much weaker functions of the volume fraction than the exponential of the barrier height. The reduced Stokes–Einstein product, or decoupling ratio, is then given by

$$\tilde{D}\tilde{\eta} = e^{\sigma_E^2} = (e^{\bar{F}_B})^{2\theta} \quad (31)$$

$$\theta \equiv \frac{\sigma_E^2}{2\bar{F}_B} \quad (32)$$

where an exponent θ is defined which quantifies the *relative* importance of the heterogeneity-induced barrier. The inset of Figure 4 shows θ is approximately constant for the high ϕ regime of interest corresponding to barriers in excess of the thermal energy. Combining eqs 31 and 32 yields

$$\tilde{D}\tilde{\eta} = (e^{(1+\theta)\bar{F}_B})^{2\theta/(1+\theta)} = \tilde{\eta}^{2\theta/(1+\theta)} \quad (33)$$

thereby implying the fractional Stokes–Einstein law

$$D \propto \eta^{-\nu}, \quad \nu = \frac{1-\theta}{1+\theta} \quad (34)$$

From Figure 4, if a simple average value of θ is employed, we analytically obtain $\nu \cong 0.71$ and 0.87 for $\xi_c/\sigma = 3$ and 4. These exponent values are in good agreement with those deduced from numerical fits to the theoretical calculations in Figure 6, i.e., $\nu \cong 0.73$ and 0.88 .

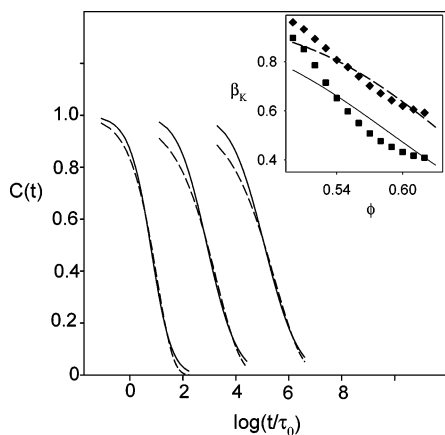


Figure 7. Relaxation function of eq 35 for $\xi_c/\sigma = 3$ and (from left to right) $\phi = 0.53, 0.58$, and 0.61 . Solid curves are the numerical results and dashed curves are the stretched exponential fits. Inset shows stretching exponents extracted from the fits $C(t)$ for $\xi_c/\sigma = 4$ (diamonds) and $\xi_c/\sigma = 3$ (squares); the analogous analytic Gaussian barrier fluctuation model exponents from eq 36 are shown as the solid and dashed curves for $\xi_c/\sigma = 3$ and 4 , respectively.

Within the context of our theory, the above results imply the fractional Stokes–Einstein law arises from mesoscopic domains associated with spontaneous density fluctuations which result in a fluctuation contribution to the barrier, $\sigma_E^2/2$. For thermal liquids, a similar conclusion has been reached based on the very different “random first-order phase transition” theory.⁴⁸ In our approach, the fluctuation part of the barrier has a dependence on the primary system control parameter, ϕ , nearly identical to that of the mean barrier, \bar{F}_B . This implies an interesting strong correlation between the “mean field” and “fluctuation” contributions to activated glassy dynamics.

Finally, following our prior work,¹⁹ full Green-Kubo calculations have been performed for the effect of domains on the self-diffusion constant and shear viscosity. We refrain from presenting more figures since, not surprisingly, the results and conclusions are essentially the same as for the simpler analytic analysis given above. Specifically, we find $\langle\eta\rangle/\bar{\eta} \cong \langle\tau\rangle/\bar{\tau}$ which is consistent with a Maxwell viscosity model²⁷ and our finding that G' is virtually unaffected by static domain disorder. The analogous result holds for the diffusion constant, $\langle D\rangle/\bar{D} \cong \langle\tau^{-1}\rangle/\bar{\tau}^{-1}$. The decoupling ratio, R , and apparent exponent ν in eq 27 are nearly identical to the full numerical volume fraction fluctuation results discussed above. For example, $\langle D\rangle\langle\eta\rangle/(\bar{D}\bar{\eta}) \cong 130$ at $\phi = 0.62$.

D. Nonexponential Relaxation. A generic relaxation function determined by *local* barrier hopping is given by

$$C(t) = \int d\phi' P(\bar{\phi} - \phi') \exp(-t/\bar{\tau}(\phi')) \cong \exp(-(t/\tau^*)^{\beta_K}) \quad (35)$$

It should be relevant to the incoherent dynamic structure factor at high wavevectors corresponding to the particle diameter or cage scale and also stress relaxation measurements. We believe it is very important that solvation dynamics,⁵² single molecule probe rotation,⁵⁰ and dielectric hole burning⁴⁹ experiments all suggest that the intradomain alpha relaxation process is “simple”. That is, the intradomain process is Gaussian and/or purely exponential time decay occurs. The stretched exponential behavior indicated by the final approximate equality in eq 35 is due to averaging over a distribution of nanoscale domains. Figure 7 shows the stretched exponential function provides a reasonable fit to our numerical results. For the Gaussian barrier

fluctuation model, the stretching exponent is accurately given by⁸

$$\beta_K \cong \frac{1}{(1 + \sigma_E^2)^{1/2}} \quad (36)$$

We find the extracted time τ^* in eq 35 is only 20–50% larger than its mean field analogue, $\bar{\tau}$, over essentially the entire range of $0.50 < \phi < 0.62$ for $\xi_c = 3$ or 4σ . The stretching exponent shown in the inset monotonically decreases with ϕ and is quite sensitive to the domain diameter. For the $\xi_c = 3\sigma$ case, $\beta_K \cong 0.50$ – 0.55 at the kinetic glass transition volume fraction of $\phi \sim 0.575$. This exponent value is close to the IMCT result^{3,4} of ~ 0.6 and also to deductions based on MCT fits of cage scale collective dynamic structure factor measurements.⁵ Rheological experiments³⁹ have reported a stretching exponent of ~ 0.5 . Note that the quoted IMCT result is valid for volume fractions below ϕ_c , whereas our theory is meant to describe the hopping dominated regime. Hence, the origin of the stretching exponent in the two theories is very different, making the apparently similar values of β_K rather surprising.

Based on the Gaussian barrier distribution model, there is a direct connection between the decoupling ratio, the stretching exponent, and the fractional Stokes–Einstein exponent. Using eqs 25, 32, 34, and 36 yields

$$R \cong e^{\sigma_E^2} \cong e^{\beta_K^{-2}-1} \quad (37)$$

$$\beta_K \cong \frac{1}{(1 + \ln(R))^{1/2}} \quad (38)$$

$$\beta_K = \frac{1}{(1 + 2\bar{F}_B(1 - \nu)(1 + \nu)^{-1})^{1/2}} \cong \frac{1}{\left(1 + (0.154S_0^{-1} - 7.02)\left(\frac{1 - \nu}{1 + \nu}\right)^{1/2}\right)} \quad (39)$$

where the second equality in eq 39 follows from using eq 7. Such inter-relationships between different measures of slow dynamics have been emphasized as a hallmark feature of glass forming liquids.¹ The stretching exponent has been advocated by Ngai as the most fundamental parameter,¹ although this interpretation is not necessary in our theory. Rather the fluctuation contribution to the collective barrier, $\sigma_E^2/2$, is the common origin of decoupling, nonexponential relaxation, and the fractional Stokes–Einstein scaling. Note that in contrast to the decoupling factor and stretching exponent in eqs 25 and 36, calculation of ν in eq 28 requires knowledge of the *relative* importance of the heterogeneity contribution to the barrier, i.e., the ratio θ .

It is important to appreciate that since $\theta \propto \sigma_E^2 \propto V_c^{-1} \propto \xi_c^{-3}$ a direct, property specific connection is suggested between the domain length scale ξ_c and the decoupling factor, fractional Stokes–Einstein exponent, and stretching exponent. This represents a strong constraint on the usefulness of a minimalist static domain model since a single (nearly) thermodynamic state independent length scale sensitively enters the determination of all “fluctuation” related quantities.

We emphasize that we have not presented a rigorous derivation of the domain size. But we do believe the results described in this section collectively demonstrate that sensible predictions for “heterogeneity effects” are obtained within a barrier hopping/static disorder theory based on a mesoscopic domain diameter of a magnitude consistent with its assumed

density fluctuation origin. Based on all of the above results, a value of $\xi_c \approx 3\sigma$ appears most consistent with experimental observations on colloidal suspensions and molecular liquids.

Finally, although most of the explicit results in this section have been obtained for colloidal suspensions, all the ideas and generic aspects of the results also apply to thermal polymer melts.^{56,57}

IV. Collective Dynamic Density Fluctuations and Heterogeneity Lifetime

The theory described in sections II and III is based on two prominent simplifications. (i) The collective many particle and single particle dynamics are controlled by the same basic hopping process in eqs 5 and 6. It appears this simplification is obeyed quite well at large wavevectors in colloidal suspensions. The reason is $q\sigma \approx 4-8$ cage scale collective relaxation times are not wavevector-dependent and have a magnitude and volume fraction dependence that is nearly identical to the slow alpha relaxation time probed in incoherent dynamic structure factor experiments.^{5,6} However, the collective and single molecule dynamic structure factors are fundamentally different on larger, supra-cage length scales. (ii) Modeling of the origin of a distribution of barriers and relaxation times as static disorder is an oversimplification, and the lifetime of the mesoscopic domain model is poorly understood.²²⁻²⁴ In our approach, addressing these two questions requires knowledge of the collective dynamic structure factor, $S(q, t)$, for long times and wavevectors $q_c \approx 2\pi/\xi_c$ well below the wide angle cage region. In this mesoscopic regime, the material is structurally homogeneous, $S(q) \sim S(0) = S_0 \ll 1$. Experiments and computer simulations generally probe the local cage scale dynamics of $S(q, t)$. We are not aware of studies in the deeply supercooled regime on the appropriate time and length scales which can definitively test our specific effectively static domain model. Hence a generic theoretical analysis is pursued.

We employ standard time-dependent statistical mechanics^{26,40} to study $S(q, t)$. On the $q_c \approx 2\pi/\xi_c$ scale, localized (beta-like) motions³⁻⁶ induce negligible decay of $S(q, t)$. The formally exact expression for the Laplace transform of the normalized dynamic structure factor in the highly viscous regime is^{40,58}

$$\frac{S(q, z)}{S(q)} = (z + q^2/[S(q)\eta_L(q, z)])^{-1} \quad (40)$$

where the generalized longitudinal viscosity is

$$\eta_L(q, t) = \beta^2 \sum_{j,k} \langle e^{iqz_j} f_j^e e^{iqz_k(t)} f_k^e(t) \rangle \quad (41)$$

In the long time, Markovian limit exponential decay occurs with a wavevector dependent collective density fluctuation relaxation time

$$S(q, t) = S(q) e^{-t/\tau_{\text{coll}}(q)} \quad (42)$$

$$\tau_{\text{coll}}(q) = q^{-2} \beta^2 S(q) \int_0^\infty dt \langle \sum_{j,k} e^{iq(z_j - z_k(t))} f_{j,j}^e f_{k,k}^e(t) \rangle \quad (43)$$

For the mesoscopic wavevectors of interest, a small q expansion is appropriate

$$\tau_{\text{coll}}(q) \cong q^{-2} S_0 D_0^{-1} + \beta^2 S_0 \int_0^\infty dt \sum_{j,k} \langle z_j f_j^e(t) f_k^e(t) \rangle \rightarrow \beta S_0 \rho^{-1} \eta_L \equiv \tau_{\text{coll}} \quad (44)$$

The leading order term in eq 44 involves the single colloid Stokes–Einstein diffusion constant, D_0 , and arises from dissipative interactions between colloids and solvent.⁴⁰ This contribution is *not* present for one-component thermal liquids. The second line in eq 44 defines the q -independent, nondiffusive collective relaxation time due to interparticle stress correlations. The nondiffusive nature follows from the momentum conservation law for direct (conservative) interparticle forces, i.e., $\sum_j f_j^e = 0$. It is surely dominant in the highly viscous regime for the nonzero, but relatively small, mesoscopic wavevectors of interest. Formally, the validity criterion is

$$\frac{2\pi^2}{3\phi} \left(\frac{\sigma}{\xi_c} \right)^2 \frac{\eta_L}{\eta_0} \gg 1 \quad (45)$$

The longitudinal viscosity is larger than the shear viscosity^{27,40}

$$\eta_L = \eta_B + (4/3)\eta_s \approx 3\eta_s \quad (46)$$

where η_B is the bulk viscosity. The final approximate equality is quite accurate for thermal liquids⁵⁹ and also follows straightforwardly from a standard MCT analysis.⁴⁰ For colloids, $\eta_s/\eta_0 \approx 30$ for $\phi \approx 0.5$,^{13,19} and hence, the left-hand side of eq 45 is $\sim 60-120$ for $\xi_c/\sigma \approx 3-4$ and increases strongly at higher volume fractions.

In the deeply “supercooled” regime ($\phi > \phi_c$, $T < T_c$), the elementary process for stress relaxation is expected to be local activated hopping. In a Maxwell model spirit, the longitudinal viscosity can be expressed as a product of its glassy plateau modulus, M' , times the activated hopping time

$$\tau_{\text{coll}} = \frac{M'}{K_B} a\langle\tau\rangle \equiv b\langle\tau\rangle \quad (47)$$

We expect the numerical prefactor $a \sim 0.5-1$, where the lower limit acknowledges the fact that local stress relaxation is related to randomizing interparticle pair separations which can occur in parallel via a hopping motion of the two particles. For colloids, the ratio of the glassy longitudinal modulus to the static bulk modulus was computed in section II (see Figure 2)

$$\Gamma \equiv \frac{M'}{K_B} \cong \frac{\pi}{6\phi} \frac{0.0124}{S_0^{1.35}} = 0.00647\phi^{-1} \left(\frac{(1+2\phi)^2}{(1-\phi)^4} \right)^{1.35} \quad (48)$$

where $\Gamma > 1$ and increases modestly from ~ 5 to 15 as $\phi \cong 0.53-0.61$. This suggests that the mesoscopic colloidal concentration fluctuations relevant to heterogeneity have a relatively long lifetime compared to the alpha relaxation time ($b > 1$), which provides some support for the effectively static domain model. New simulations that determine the parameter b would be valuable.

For thermal liquids, ultrasonic,⁶⁰ impulsive light scattering,⁶¹ and mechanical⁵⁹ experiments suggest the factor b in eq 47 is of the order of unity and increases weakly with cooling. The latter trend might be interpretable in terms of eq 47 since the high-frequency M' is known to be more temperature dependent⁶² than the bulk modulus K_B . A value of $b \sim 1$ seems consistent with NMR^{22,42} and some dielectric⁵³ measurements on molecular liquids near T_g . However, other experiments,^{22-24,50-52} generally involving rotation or translation of probe molecules, find the exchange or heterogeneity time is much longer than the alpha relaxation time. Since the latter experiments probe a

different process, often in a different manner, there may be no contradiction.

V. Incoherent Structure Factor and a Dynamic Heterogeneity Length Scale

The single molecule, or incoherent, dynamic structure factor, $F(q, t)$, has been widely studied by simulations^{1,2,14,15} and dynamic light scattering (DLS) in colloidal suspensions.⁶ The focus is usually on large wavevectors that probe the local cage dynamics. Here we are interested in the mesoscopic wavevector regime. As is well-known,²⁶ the incoherent dynamic structure factor probes diffusive translational dynamics as $q \rightarrow 0$ in strong contrast to its collective analogue $S(q, t)$.

The two-point incoherent dynamic structure factor is given by²⁶

$$F(q, t) = \langle e^{i\vec{q} \cdot (\vec{r}(t) - \vec{r}(0))} \rangle \rightarrow e^{-t/\tau_D(q)} \quad (49)$$

where the second line applies in the long time Markovian limit. The formally exact expression for the single particle wavevector-dependent relaxation time is^{26,40}

$$\tau_D(q) = q^{-2} \beta^2 \int_0^\infty dt \langle \sum_j e^{iq(z_j - z_j(t))} f_{jj}(t) \rangle \quad (50)$$

In the mesoscopic regime, a small wavevector expansion is appropriate, which yields

$$\frac{1}{\tau_D(q)} = \frac{q^2 D}{1 + (q\xi_D)^2} \quad (51)$$

Here, ξ_D is a “diffusive dynamic correlation length”, and D is the ensemble-averaged long time self-diffusion constant. The length ξ_D is fundamentally distinct from the (model dependent) domain diameter, ξ_c , employed in section III that quantified the (effectively static) scale on which an intradomain cooperative barrier hopping process occurs. The form of eq 51 is identical to venerable, and largely empirical, “jump diffusion” models²⁶ for local single particle dynamics where $\xi_D \approx \sigma$. The dynamic correlation length follows from eqs 50 and 51 as

$$\xi_D^2 = \rho^{-1} \beta D \eta_L^s \cong 3\rho^{-1} \beta D \eta_s^s \quad (52)$$

where η_L^s (η_s^s) is the single molecule analogue of the longitudinal (shear) viscosity (eq 44) which contains only time correlations between stresses on the *same* molecule or colloid. The final approximate equality employs the analogue of eq 46 and follows from a standard MCT factorization and projection analysis.^{3,40} In principle, the single molecule version of the shear viscosity in eq 52 is not the same as the (collective) shear viscosity, but it is difficult to imagine they are very different if activated dynamics is dominant. Some evidence for this claim follows from applying our prior Green-Kubo based theory for the collective shear viscosity of hard sphere suspensions to the calculation of η_s^s .¹⁹ The slow variable that is now projected onto is a bilinear product of the single particle and collective density fields instead of a product of collective density fields.⁴⁰ The analogues of eqs 9–11 are easily written down for η_s^s . The ratio of the single particle and collective shear viscosities (excluding the unimportant high-frequency part) is then given by

$$X \equiv \frac{\eta_s^s}{\eta_s} = \frac{\int_0^\infty dq q^2 \left(\frac{\partial}{\partial q} \ln S(q) \right)^2 2S(q)(1 + S^{-1}(q))^{-1}}{\int_0^\infty dq q^2 \left(\frac{\partial}{\partial q} \ln S(q) \right)^2 S(q)} \quad (53)$$

Since the viscosity is dominated by high wavevector contributions, X cannot deviate from unity by a large amount. Numerical calculations show it weakly decreases from ~ 1 to ~ 0.6 as volume fraction increases from 0.5 to 0.6.

The diffusive dynamic correlation length is now expressible in terms of commonly *measured* quantities

$$\xi_D^2 = 3X\rho^{-1} \beta D \eta_s^s = \sigma^2 \left(\frac{\pi}{2\phi} X \beta \sigma D \eta_s^s \right) \quad (54)$$

Physically, ξ_D can be interpreted as the characteristic distance a colloid or molecule must diffuse before random Fickian diffusion applies. It sometimes is referred to as a “viscoelastic” length since it describes the finite length scale influence of stress fluctuations on translational motion. In liquids far from a glass transition, ξ_D is on the order of the molecular size. This is easily seen by rewriting eq 54 as

$$\xi_D \cong \sigma \left(\frac{X}{6\phi} \right)^{1/2} \left(\frac{D \eta_s^s}{(D \eta_s^s)_{SE}} \right)^{1/2} = \xi_{D,\infty} (R_D)^{1/2} \quad (55)$$

where eq 26 has been used, and the high-temperature limit is defined as $\xi_{D,\infty}$ which is proportional to the cube root of molecular volume. Equations 49 and 51 imply Fickian diffusion is obtained only on length scales that obey $q\xi_D \ll 1$. For smaller length scales where $q\xi_D \gg 1$, the single particle dynamics is nonFickian, and the relaxation rate of $F(q, t)$ is wavevector independent. An equivalent statement is the length scale dependent diffusion constant, defined from $F(q, t) \equiv \exp(-D(q)q^2t)$, follows an inverse square law

$$D(q) \approx \frac{D}{(q\xi_D)^2}, \quad q\xi_D \gg 1 \quad (56)$$

This is a hallmark of nondiffusive dynamics which emerges as a *generic* consequence of a large viscoelastic length. The latter is realized on mesoscopic scales only if there is a strong violation of the Stokes–Einstein law, $R_D \gg 1$. Note that none of this discussion involves complicated multipoint dynamic correlation functions often invoked to describe “dynamic heterogeneity”.^{22–24,42} Length scales extracted from them are presumably not identical to ξ_D , but we suspect they are closely related.

We now consider the magnitude of the diffusive dynamic correlation length for colloidal suspensions. For a representative value of $X \sim 0.8$ and a domain diameter of 3 particle diameters, eq 55 yields $\xi_D/\sigma \cong 1.5$ at the kinetic glass transition $\phi \approx 0.57$. This small length scale seems consistent with the observation of a Gaussian wavevector dependence of $F(q, t)$.⁶ On the other hand, at a high “glassy” concentration of $\phi \approx 0.62$ one finds $\xi_D/\sigma \cong 5.7$. These results are not unexpected since, as discussed in section III, large decoupling factors require very high relative viscosities which is not the situation for colloidal volume fractions typically studied by DLS and rheology.

The above generic analysis also applies to molecular and other thermal liquids. For tri-naphthyl-benzene, experiments⁵⁵ find $R_D \sim 400$ at T_g . The molecular diameter of TNB is ~ 1 nm, and a typical liquid volume fraction corresponds to $\phi \sim 0.5$. Substituting these numbers in eq 55 yields a dynamic correlation length of $\xi_D \cong 10$ nm. This remarkably large number significantly exceeds our $\xi_c \cong (3-4)\sigma$, or the typical domain size or

dynamic heterogeneity length of $\approx 2\text{--}4$ nm as deduced from NMR and other indirect experiments.^{22–24} This difference is perhaps not unexpected since, as emphasized by Ediger,⁶³ ξ_D is the *ensemble-averaged* length beyond which the single molecule diffusion process is homogeneous, which requires traversal of multiple “domains” resulting in $\xi_D > \xi_c$ at low temperatures. Moreover, in contrast to ξ_c , the diffusive dynamic correlation length strongly decreases with heating since the decoupling factor is very temperature dependent and approaches unity at T_c where ξ_D becomes of the order of, or smaller than, the molecular diameter. Hence, the observation of a q -dependent diffusion constant, and a large and temperature dependent (but *not* divergent) dynamic length scale in $F(q,t)$, is a *direct and generic* consequence of strong translation-rotation/viscosity decoupling.

There is also the question of the time scale associated with the incoherent dynamic scattering experiment versus an average alpha relaxation time. If $F(q,t)$ is measured in the $q\xi_D \gg 1$ “heterogeneous” regime, then the relaxation time is given from eq 51 as

$$\tau_D = \frac{\xi_D^2}{D} = \sigma^2 \frac{\pi}{2\phi} \beta \sigma \eta_s \approx \langle \tau \rangle \left(\frac{a\pi}{2\phi} \right) \left(\frac{G_\infty}{k_B T \sigma^{-3}} \right), \quad q\xi_D \gg 1 \quad (57)$$

where the final approximate equality follows from using the Maxwell viscosity relation,⁶⁴ $\eta_s \approx G_\infty \langle \tau \rangle$, with a high-frequency shear modulus which is an upper bound on the glassy modulus. The time τ_D can be compared to various measures of a mean alpha relaxation time. For a 1 nm molecule, $k_B T \sigma^{-3} \sim 4.2 \times 10^6$ Pascals at room temperature, and typical values of the high frequency modulus in the deeply supercooled regime are $\sim 10^8\text{--}10^9$ Pascals.^{62,64} Hence, the diffusive relaxation time is typically a factor of 25–250 times larger than the mean alpha relaxation time. The ratio $\tau_D/\langle \tau \rangle$ significantly increases with cooling since $\beta G_\infty(T)$ is a decreasing function of temperature.⁶²

Equation 57 can alternatively be written as

$$\tau_D = \frac{\sigma^2}{D} \frac{X}{6\phi} R_D \equiv \tau_F \frac{X R_D}{\phi}, \quad q\xi_D \gg 1 \quad (58)$$

where a Fickian diffusion time associated with local hopping, τ_F , is defined in a standard manner. The time τ_D is a factor of $\sim X R_D/\phi$ larger than this local Fickian diffusion time and is strongly temperature-dependent. Finally, the diffusive time τ_D can be compared to the “most probable” alpha relaxation time defined as τ^* in eq 35 which is often extracted from DLS or dielectric measurements. Based on the hard sphere calculations in section III, τ^* is only slightly larger than the rigorously most probable mean time, $\bar{\tau}$. Hence, we estimate

$$\frac{\tau_D}{\tau^*} \approx \frac{\tau_D}{\bar{\tau}} \approx (R_D)^{1/2} \frac{\tau_D}{\langle \tau \rangle} \quad (59)$$

where the final approximate equality follows from using the Gaussian distributed barrier model. From the discussion below eq 57, this time scale ratio is $\sim 250\text{--}2500$ for a decoupling ratio of $R_D \sim 100$.

The large ratios of the diffusive time characterizing the onset of Fickian behavior in $F(q,t)$ to various measures of the alpha relaxation time seem qualitatively consistent with probe-based single molecule rotation, deep bleach, and solvation relaxation experiments.^{22–24,49–52} The ratio is large since τ_D characterizes a mass transport process in contrast to the average alpha relaxation time which generally reflects a nondiffusive relaxation

of stress or orientation within a domain. Experiments in progress⁶³ should allow testing of the theoretical results in this section.

Many questions remain to be definitively answered, including the following. (i) How is the experimentally measured “heterogeneity lifetime” or “exchange time”^{22–24} related to τ_D , τ_{coll} , $\langle \tau \rangle$, or other times? (ii) Is the recovery of ergodicity, including long time exponential decay of $C(t)$ and the effective collapse of the density fluctuation distribution of eq 19 to a delta function, controlled by single particle mass transport (diffusion) or collective dynamics? (iii) What is the (property specific) relevant length scale for ergodicity to be achieved, ξ_c , ξ_D , or some other length?

Finally, we mention recent theoretical work based on highly coarse grained kinetic facilitated Ising models (FIM) and complementary molecular dynamics simulation studies of *weakly* supercooled fluids, which have addressed some of the above issues.^{30,65,66} Evidence has been obtained^{65,66} for power law connections between a growing time scale, τ , a growing dynamic length scale, l , and translation-rotation decoupling

$$l \approx \tau^{1/z}, \quad D \approx \eta^{-1+(\beta/z)} \quad (60)$$

Simulations of two and multi-point time correlations of simple atomic mixtures find $z^{-1} \approx 0.22$ and $\beta/z \approx 0.35$, whereas a renormalization group calculation and various versions of facilitated Ising models find similar scaling with a variety of exponents.^{65,66} A result analogous to eq 56 is obtained for $ql \gg 1$ but with $D(q) \sim (ql)^{-\beta}$ and $\beta \approx 1.6$. A field theoretic analysis⁶⁷ of a schematic MCT-like theory has also found a power law relation between a dynamic length and time scale. However, in contrast to our theory and the FIM studies, there are divergences at nonzero temperature.

Note that if one accepts decoupling in the sense $D \approx \eta^{-\nu}$, then eqs 54 and 57 immediately imply a connection between our time and length scales

$$\xi_D \approx \tau_D^{(1-\nu)/2} \quad (61)$$

From the perspective of our analysis of $F(q,t)$, a time–length scale relation as in eq 60 seems inevitable and model independent. Specification of the exponent(s) requires a specific physical model or idea. This issue was addressed in section IIIC for colloids and elsewhere for polymer melts.⁵⁷

VI. Summary and Discussion

Our microscopic entropic barrier hopping theory of slow single particle dynamics in hard sphere colloidal suspensions^{18,19} has been extended to include effectively static heterogeneity. The origin of local domains, their size, and the corresponding barrier fluctuations are attributed to mesoscopic density fluctuations of an amplitude controlled by the isothermal compressibility. The typical domain size that determines barriers and the activated hopping rate is estimated to be 3–4 particle diameters, and only weakly dependent on volume fraction or temperature. Interestingly, this length scale is consistent with experimental estimates^{22–24} of various dynamic heterogeneity or cooperativity length scales in molecular and polymer liquids close to T_g . As a first approximation, the mesoscopic density fluctuations are treated as inducing static disorder. Consequences include an increase of the ensemble-average relaxation time and diffusion constant, stretched exponential decay of local dynamic correlators, translation-viscosity decoupling, and a fractional Stokes–Einstein relation. These non-mean-field effects are material-

specific and have a common origin: the fluctuation induced component of the barrier. Surprisingly, the latter depends on colloid volume fraction in a nearly identical manner as the mean barrier does. This suggests a close correlation and common origin of the mean field (average) and heterogeneity (fluctuation) aspects, which we find also applies to thermal polymer melts.^{56,57} For suspensions and volume fractions in the dynamical precursor regime, the barrier fluctuations have modest consequences, except for the question of nonexponential relaxation. Predictions are made for volume fractions in the putative glassy regime where the effects are significantly larger.

A statistical dynamic analysis of the lifetime of density fluctuation based domains has been presented which is relevant to colloidal suspensions and deeply supercooled liquids. For suspensions, the relaxation time of collective density fluctuations on the mesoscopic scale is estimated to be at least as long as the single particle hopping time, and perhaps an order of magnitude larger. For thermal liquids, the analysis suggests the heterogeneity lifetime is at least comparable with the mean α relaxation time. If the lifetime of the domain structures is comparable to or shorter than the mean α time, then heterogeneity effects will be reduced (dynamic averaging), and a fully self-consistent treatment of $\langle \tau \rangle$ and τ_{coll} should be pursued. This aspect is particularly important for the dynamics of relatively large, slowly rotating probes dissolved in supercooled liquids.^{22–24}

A general, model-independent analysis of the incoherent dynamic structure factor in the long time and intermediate wavevector regime has been performed. Coupling of single particle density fluctuations (mass transport) and longitudinal stress fluctuations result in nonFickian behavior, a wavevector-dependent apparent diffusion constant, and a diffusive dynamic correlation (or viscoelastic) length scale that is strongly temperature dependent but not divergent. The growing length scale is directly correlated with the degree of translation–rotation decoupling. It is estimated to be 10 times larger than a molecular diameter for TNB near the thermal glass transition, but shrinks to a molecular size or smaller above (below) the crossover temperature (volume fraction) that signals the emergence of collective barriers.^{18,56}

Finally, calculations of the modulus, entropic barrier, and other properties of colloidal suspensions show the strong dependences on volume fraction are remarkably well correlated with the inverse compressibility or bulk modulus. Since the latter is a long wavelength or thermodynamic measure of the amplitude of density fluctuations, this suggests that a surprising “coarse-graining” process may be operative in the hopping controlled regime. We have extended our ideas to develop a coarse-grained theory of slow segmental dynamics, heterogeneity, and the glass transition in polymer melts.^{56,57,67} Generalization to treat molecular fluids and liquid metals is in progress and will be reported elsewhere.⁶⁸

Acknowledgment. This paper is dedicated to Frank Stillinger in honor of his many outstanding and pioneering contributions to statistical mechanics and the theory of liquids. Stimulating and informative discussions and correspondence with Professor Mark Ediger concerning the glass transition in general and our theoretical work are gratefully acknowledged. K.S.S. is particularly grateful for detailed discussions with Professor Ediger concerning his preliminary measurements of the incoherent dynamic structure factor of molecular liquids and the associated physics. We thank Dr. Vladimir Kobelev for performing the calculations of X in eq 53. The colloidal suspension part of this work was supported by the Nanoscale Science and

Engineering Initiative of the National Science Foundation under NSF Award Number DMR-0117792. Support for the thermal glass forming liquid aspects is from the United States Department of Energy, Division of Materials Science under Award Number DEFG02-91ER45439, through the Frederick Seitz Materials Research Laboratory at the University of Illinois at Urbana-Champaign.

References and Notes

- (1) For recent reviews see the following, Ngai, K. L. *J. Non-Cryst. Sol.* **2000**, 275, 7. Angell, C. A.; Ngai, K. L.; McKenna, G. B.; McMillan, P. F.; Martin, S. W. *J. Appl. Phys.* **2000**, 88, 3113.
- (2) Debenedetti, P. G.; Stillinger, F. H. *Nature* **2001**, 410, 259.
- (3) Gotze, W.; Sjogren, L. *Rep. Prog. Phys.* **1992**, 55, 241. Gotze, W. *J. Phys. Condensed Matter* **1999**, 11, A1.
- (4) Fuchs, M.; Hofacker, I.; Latz, A. *Phys. Rev. A* **1992**, 45, 898.
- (5) van Megen, W.; Underwood, S. *Phys. Rev. E* **1994**, 49, 4206.
- (6) van Megen, W.; Mortensen, T. C.; Williams, S. R. *Phys. Rev. E* **1998**, 58, 6073.
- (7) Stickel, F.; Fischer, E. W.; Richert, R. *J. Chem. Phys.* **1995**, 102, 6251.
- (8) Monthus, C.; Bouchaud, J. P. *J. Phys. A* **1996**, 29, 3847. Bouchaud, J. P.; Cugliandolo, L.; Kurchan, J.; Mezard, M. *Physica A* **1996**, 226, 243.
- (9) Dyre, J. C. *Phys. Rev. Lett.* **1987**, 58, 792. Dyre, J. C. *Phys. Rev. B* **1995**, 51, 12276.
- (10) Arkhipov, V. I.; Bassler, H. *Phys. Rev. E* **1995**, 52, 1227. Bassler, H. *Phys. Rev. Lett.* **1987**, 58, 767.
- (11) Evans, R. M. L.; Cates, M. E.; Sollich, P. *Eur. Phys. J. B* **1999**, 10, 705.
- (12) Pusey, P. N. in *Liquids, Freezing and the Glass Transition*; Hansen, J. P., Levesque, D., Zinn-Justin, J., Eds.; North-Holland: Amsterdam, 1991.
- (13) Cheng, Z.; Zhu, J.; Chaiken, P. M.; Phan, S. E.; Russel, W. B. *Phys. Rev. E* **2002**, 65, 041405.
- (14) Kob, W. *J. Phys. Condens. Matter* **1999**, 11, R85.
- (15) Binder, K. *J. Non-Cryst. Sol.* **2000**, 274, 332.
- (16) Weeks, E. R.; Weitz, D. A. *Phys. Rev. Lett.* **2002**, 89, 095704. Weeks, E. R.; Weitz, D. A. *Chem. Phys.* **2002**, 284, 361. Weeks, E. R.; Crocker, J. C.; Levitt, A.; Schofield, A.; Weitz, D. *Science* **2000**, 287, 627.
- (17) Kasper, A.; Bartsch, E.; Sillescu, H. *Langmuir* **1998**, 14, 5004.
- (18) Schweizer, K. S.; Saltzman, E. J. *J. Chem. Phys.* **2003**, 119, 1181.
- (19) Saltzman, E. J.; Schweizer, K. S. *J. Chem. Phys.* **2003**, 119, 1197.
- (20) Denny, R. A.; Reichman, D. R.; Bouchaud, J. P. *Phys. Rev. Lett.* **2003**, 90, 025503. Brumer, Y.; Reichman, D. R. *Phys. Rev. E* **2004**, 69, 041202.
- (21) Doliwa, B.; Heuer, A. *Phys. Rev. E* **2003**, 67, 030501. Doliwa, B.; Heuer, A. *Phys. Rev. E* **2003**, 67, 030506.
- (22) Ediger, M. *Annu. Rev. Phys. Chem.* **2000**, 51, 99.
- (23) Richert, R. *J. Phys. Condens. Matter* **2002**, 14, R703.
- (24) Sillescu, H. *J. Non-Cryst. Sol.* **1999**, 243, 81.
- (25) Kirkpatrick, T. R.; Wolynes, P. G. *Phys. Rev. A* **1987**, 35, 3072.
- (26) Hansen, J. P.; McDonald, I. R. *Theory of Simple Liquids*; Academic Press: London, 1986.
- (27) Russel, W. B.; Saville, D. A.; Schowalter, W. R. *Colloidal Dispersions*; Cambridge University Press: Cambridge, U.K., 1989.
- (28) Lionberger, R. A.; Russel, W. B. *J. Rheol.* **1994**, 38, 1885.
- (29) Oxtoby, D. In *Liquids, Freezing and the Glass Transition*; Hansen, J. P., Levesque, D., Zinn-Justin, J., Eds.; North-Holland: Amsterdam, 1991.
- (30) Ritort, F.; Sollich, P. *Adv. Phys.* **2003**, 52, 219. Whitlam, S.; Garrahan, J. P. *J. Phys. Chem. B* **2004**, 108, 6611.
- (31) Rintoul, M. D.; Torquato, S. *J. Chem. Phys.* **1996**, 105, 9258. Torquato, S.; Truskett, T. M.; Debenedetti, P. G. *Phys. Rev. Lett.* **2000**, 84, 2064. Kansal, A. R.; Torquato, S.; Stillinger, F. H. *Phys. Rev. E* **2002**, 66, 041109.
- (32) Kramers, H. A. *Physica* **1940**, 7, 284.
- (33) Cohen, E. G. D.; Verberg, R.; de Schepper, I. M. *Physica A* **1998**, 251, 251.
- (34) Chen, Y. L.; Schweizer, K. S. *J. Chem. Phys.* **2004**, 120, 7212.
- (35) Mason, T. G.; Gang, H.; Weitz, D. A. *J. Opt. Soc. Am. A* **1997**, 14, 139.
- (36) Kobelev, V.; Schweizer, K. S. *Phys. Rev. E* submitted.
- (37) Petekidis, G.; Vlassopoulos, D.; Pusey, P. *Faraday Discuss.* **2003**, 123, 287.
- (38) Nommensen, P. A.; Duits, M. H. G.; van den Ende, D.; Mellema, J. *Phys. Rev. E* **1999**, 59, 3147.
- (39) Marshall, L.; Zukoski, C. F. *J. Phys. Chem.* **1990**, 94, 1164.
- (40) Hess, W.; Klein, R. *Adv. Phys.* **1983**, 32, 173.
- (41) Koshy, R.; Desai, T.; Keblinski, P.; Hooper, J.; Schweizer, K. S. *J. Chem. Phys.* **2003**, 119, 7599.
- (42) Tracht, U.; Wilhelm, M.; Heuer, A.; Spieiss, H. W. *J. Magn. Reson.* **1999**, 140, 460.

- (43) Qiu, X.; Ediger, M. D. *J. Phys. Chem. B* **2003**, *107*, 459.
- (44) Lodge, T. P.; McLeish, T. C. B. *Macromolecules* **2000**, *33*, 5278.
- (45) Kant, R.; Kumar, S. K.; Colby, R. H. *Macromolecules* **2003**, *36*, 10087.
- (46) Moynihan, C. T.; Schroeder, J. J. *Non-Cryst. Sol.* **1993**, *160*, 52.
- Ediger, M. D. *J. Non-Cryst. Sol.* **1998**, 235, 10.
- (47) Donth, E. *J. Non-Cryst. Sol.* **1982**, *53*, 325. Chamberlin, R. *Phys. Rev. Lett.* **1999**, *82*, 2520.
- (48) Xia, X.; Wolynes, P. G. *Phys. Rev. Lett.* **2001**, *86*, 5526. Xia, X.; Wolynes, P. G. *Proc. Nat. Acad. Sci.* **2000**, *97*, 2990.
- (49) Jeffrey, K. R.; Richert, R.; Duvvuro, K. J. *Chem. Phys.* **2003**, *119*, 6150.
- (50) Deschenes, L. A.; Vanden Bout, D. A. *J. Phys. Chem. B* **2002**, *106*, 11438. Deschenes, L. A.; Vanden Bout, D. A. *Science* **2001**, *292*, 255.
- (51) Cicerone, M. T.; Ediger, M. D. *J. Chem. Phys.* **1993**, *97*, 10489.
- (52) Wendt, H.; Richert, R. *Phys. Rev. E* **2000**, *61*, 1722.
- (53) Russel, E. V.; Israeloff, N. E. *Nature* **2000**, *408*, 695.
- (54) Novikov, V. N.; Sokolov, A. P. *Phys. Rev. E* **2003**, *67*, 031507.
- (55) Swallen, S. F.; Bonvallet, P. A.; McMahon; R. J.; Ediger, M. D. *Phys. Rev. Lett.* **2003**, *90*, 015901.
- (56) Schweizer, K. S.; Saltzman, E. J. *J. Chem. Phys.* **2004**, *121*, 1984.
- (57) Saltzman, E. J.; Schweizer, K. S., manuscript in preparation.
- (58) Schweizer, K. S. *J. Chem. Phys.* **1989**, *91*, 5822.
- (59) Angell, C. A.; Bohmer, R., unpublished manuscript available on the website of Angell, C.; Cutroni, M.; Mandanici, A. *J. Chem. Phys.* **2001**, *114*, 7124.
- (60) Meister, R.; Marhoeffer, C.; Sciamanda, R.; Cotter, L.; Litovitz, T. *J. Appl. Phys.* **1960**, *31*, 854 and references therein.
- (61) Silence, S.; Duggal, A. R.; Dahr, L.; Nelson, K. M. *J. Chem. Phys.* **1992**, *96*, 5448.
- (62) Dyre, J. C.; Olsen, N. B.; Christensen, T. *Phys. Rev. B* **1996**, *53*, 2171.
- (63) Ediger, M. D. private communication.
- (64) Larson, R. G. *The Structure and Rheology of Complex Fluids*; Oxford University Press: New York, 1999.
- (65) Garrahan, J. P.; Chandler, D. *Proc. Natl. Acad. Sci.* **2003**, *100*, 9710. Garrahan, J. P.; Chandler, D. *Phys. Rev. Lett.* **2002**, *89*, 035704. Jung, Y.; Garrahan, J. P.; Chandler, D. *Phys. Rev. E* **2004**, *69*, 061205.
- (66) Berthier, L. *Phys. Rev. E* **2004**, *69*, 020201. Whitelam, S.; Berthier, L.; Garrahan, J. P. *Phys. Rev. Lett.* **2004**, *92*, 185705.
- (67) Biroli, G.; Bouchaud, J. P. *Europhys. Lett.* **2004**, *67*, 21.
- (68) Saltzman, E. J.; Schweizer, K. S. *J. Chem. Phys.* **2004**, *121*, 2001.
- (69) Saltzman, E. J.; Schweizer, K. S., to be submitted.